Experimental verification of Rayleigh scattering cross sections

Hans Naus and Wim Ubachs

Department of Physics and Astronomy, Vrije Universiteit, De Boelelaan 1081, 1081 HV Amsterdam, The Netherlands

The cavity-ringdown technique is applied to measure Rayleigh extinctions of Ar, N_2, and SF_6 in the 560–650-nm region at 294 K. It is shown that experimental and calculated Rayleigh scattering cross sections agree within an experimental uncertainty of 1% (for SF_6, 3%).   © 2000 Optical Society of America

OCIS codes: 290.5870, 290.5840.

A century ago Lord Rayleigh formulated a theory of light scattering by ideal gases that not only explained the molecular origin of atmospheric scattering and the blue color of the clear sky but also provided a quantitative expression for the amount of light scattered.[1] In modern formulation the Rayleigh scattering cross section $\sigma_{(\nu)}$ [cm^2] for a single molecule is given by[2–4]

$$\sigma_{(\nu)} = \frac{24\pi^3 \nu^4}{N^2} \frac{[n_{(\nu)}^2 - 1]^2}{[n_{(\nu)}^2 + 2]^2} F_{k(\nu)}, \qquad (1)$$

where ν is the frequency [cm^{-1}], N is the molecular density [cm^3], $n_{(\nu)}$ is the refractive index, and $F_{k(\nu)}$ is the King correction factor.   The factor $[n_{(\nu)}^2 - 1]/[n_{(\nu)}^2 + 2]$, an effect of the local electrostatic field that is known as the Clausius–Mossotti or the Lorentz–Lorenz factor, is proportional to N. Because of this proportionality one must be consistent in choosing the values of $n_{(\nu)}$ and N. The King correction factor is defined as $F_{k(\nu)} = (6 + 3\rho_n)/(6 - 7\rho_n)$, where ρ_n is the depolarization ratio of natural or unpolarized light and accounts for the anisotropy of nonspherical molecules.[5]

Equation (1) includes effects of nonresonant scattering that were unknown to Rayleigh; the fine structure on the Rayleigh line is related to vibrational and rotational Raman scattering, the influence of the modes of hypersound is known as Brillouin scattering, and the effects of collisional redistribution give rise to Rayleigh wing scattering.

Hence Rayleigh scattering cross sections follow directly from the theory of electromagnetism, with N, $n_{(\nu)}$, and ρ_n as relevant parameters. N involves knowledge of Avogadro's number, and values of $[n_{(\nu)} - 1]$ can be measured to high accuracy by interferometric techniques[6] or can be calculated in terms of molecular polarizability. The depolarization ρ_n can be determined from studies of the rotational Raman effect.[7,8] With known parameters, $\sigma_{(\nu)}$ can be calculated with accuracies of 1% for N_2 and 0.3% for Ar. The uncertainties originate from the accuracy of $n_{(\nu)}$ and, in the case of N_2, $F_{k(\nu)}$.

In the present experiment a linearly polarized laser was used. Although for polarized light the depolarization ratio ρ_v is different,[8,9] i.e., $\rho_n = 2\rho_v/(1 + \rho_v)$, the King factor that enters the equation for the cross section is not dependent on the polarization state of the incident beam, as is clear from symmetry.

Accurate tabulations of frequency-dependent Rayleigh scattering coefficients for air have been produced based on electromagnetic theory and measurements of $n_{(\nu)}$ and ρ_n. The tables presented by Bucholtz,[2] Bates,[3] and Penndorf[10] are often used in atmospheric optics. It is probably for this reason that calculations of these coefficients have to our knowledge never been subjected to a laboratory test; moreover, a measurement of scattered intensity requires accurate knowledge of both the optical-collection and the quantum efficiencies of a detector. Hence a direct quantitative measurement of the scattered light is impractical. However, in the absence of absorption, scattering is equal to extinction. Based on this assumption, we performed measurements of the Rayleigh scattering cross section by monitoring extinction with the cavity-ringdown (CRD) technique.

The CRD setup was described in detail previously.[11] A laser pulse is coupled into a stable nonconfocal cavity consisting of two highly reflecting curved mirrors. The intensity of the light leaking out of the cavity will decrease exponentially in time.[12] The decay rate is determined by the reflectivity of the mirrors and the losses in the cavity that are due to absorption or scattering. Under the condition that the additional losses obey Beer's law, the decay rate $\beta_{(\nu)}$ is described by

$$\beta_{(\nu)} = \frac{c}{d} |\ln(R)| + \frac{c}{d} \sigma_{(\nu)} lN, \qquad (2)$$

where c is the speed of light, d is the cavity length, R is the reflectivity of the mirrors, and l is the length of the scattering medium. If the medium fills the cavity ($d = l$), the slope of the decay rate $\beta_{(\nu)}$ as a function of pressure yields the scattering cross section, independent of the cavity length. This is a marked advantage of the CRD technique.

Light emerging from the cavity is detected with a photomultiplier tube; transients are stored on a digital oscilloscope and fitted on line to an exponential function by computer. Reliable determination of the cavity loss requires monoexponential decay. The cavity is aligned by on-line monitoring of fit parameters and residues to achieve monoexponential behavior over the total decay. Decay rates $\beta_{(\nu)}$ are determined by use of a summation over three laser pulses. Decay times τ [$=1/\beta_{(\nu)}$] of 15–85 μs fitted over $\approx 5\tau$ correspond to path lengths of 20–125 km in the 80-cm-long

cell. This is another advantage of CRD: Long path lengths can be obtained in a short cell, yielding high sensitivities, on average 5×10^{-9} cm^{-1} for this setup.

While transients are recorded at a fixed laser frequency, the gas pressure in the CRD cell is gradually increased from 0 to 750 Torr by means of a needle valve tap. Two buffer chambers with multiple outlets welded to the tube over the total length of the CRD cell ensure a homogeneous gas pressure. Before the gas (Ar$_3$, N$_2$, or SF$_6$ of 99.999% purity) enters the cell it is purged through a 0.5-μm sintered stainless-steel filter. The pressure, measured by a capacitance manometer (Edwards 600 AB; 0.15% accuracy), is simultaneously recorded with the decay transients. To cover the frequency range we use a tunable pulsed dye laser system of 0.05-cm^{-1} bandwidth and 5-ns pulse duration. Calibration against the I$_2$ reference standard results in an absolute frequency accuracy of better than 0.1 cm^{-1}.

Figure 1 shows the measured cavity losses $[\beta_{(\nu)}/c]$ in Ar, N$_2$, and SF$_6$ as a function of pressure at 579.82 nm. The curves typically consist of 1500 data points. The difference between the extinction of Ar and N$_2$ is clearly visible. The extinction of SF$_6$ is an order of magnitude larger, reflecting the large refractive index of SF$_6$. A linear regression reveals the slope or Rayleigh extinction rate [cm^{-1} Torr^{-1}], from which the scattering cross section can be determined. The intercept represents the loss of the empty cavity. The residue of an unweighted linear regression (Fig. 1, bottom panel) of the Ar extinction curve confirms the linear behavior of the extinction as a function of the pressure and gives an impression of the sensitivity.

The Rayleigh scattering cross sections of Ar and N$_2$, determined from the extinction rates, are plotted in Fig. 2 as a function of frequency. The experimentally determined cross sections are compared with calculations based on Eq. (1). The well-known refractive indices for Ar and N$_2$ are invoked.[3,6] Ar is a spherical particle, but N$_2$ is a diatom for which a depolarization has to be taken into account[3]:

$$F_{k(\nu)} = 1.034 + 3.17 \times 10^{-12} \nu^2. \qquad (3)$$

The calculated cross sections $\sigma_{(\nu)}$ are displayed as solid curves in Fig. 2.

Light scattered in the forward and backward directions does not give rise to extinction in the CRD experiment, resulting in underestimation of the true scattering cross section. However, with effective reflection surfaces of 5-mm diameter and mirrors separated by 80 cm, imposing the stability criterion for the cavity and accounting for the nonisotropic scattering distribution, we find that the underestimate is less than 0.05%. These effects are therefore neglected.

For quantitative verification the obtained data on the cross section $\sigma_{(\nu)}$ are fitted to a functional form. Since the Rayleigh scattering cross section deviates from a ν^4 behavior owing to the frequency dependence of the refractive index and the depolarization, it is usually expressed as[13]

$$\sigma_{(\nu)} = \bar{\sigma} \nu^{4+\epsilon}. \qquad (4)$$

The measurements span a relatively small frequency domain, which results in a strong correlation between the experimentally determined value $\bar{\sigma}_{\mathrm{exp}}$ and ϵ in a two-parameter fit. To determine reliable values for $\bar{\sigma}_{\mathrm{exp}}$ we choose to keep ϵ fixed at values following from calculations according to Eq. (1). Values of $\bar{\sigma}_{\mathrm{exp}}$ as well as calculated values for $\bar{\sigma}_{\mathrm{th}}$ and ϵ [from Eq. (1)]
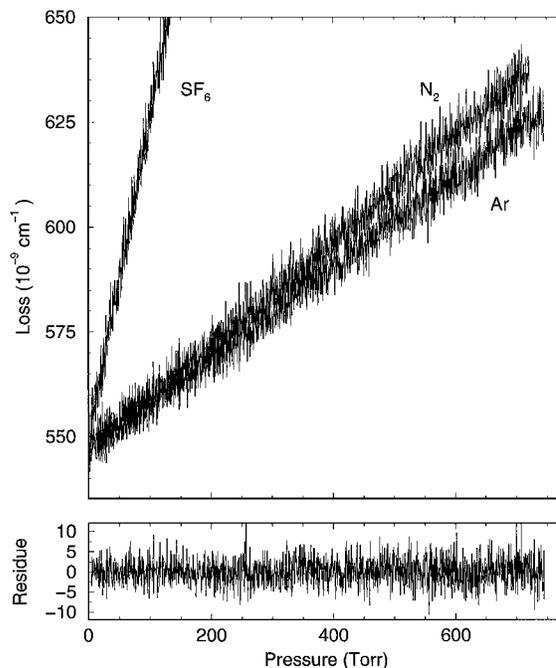

Fig. 1. Extinction owing to Ar, N$_2$, and SF$_6$ as a function of pressure measured in the CRD setup. The bottom panel shows the residue of an unweighted linear regression of the Ar extinction curve (rms, 3×10^{-9} cm^{-1}; mean, 4×10^{-13} cm^{-1}).
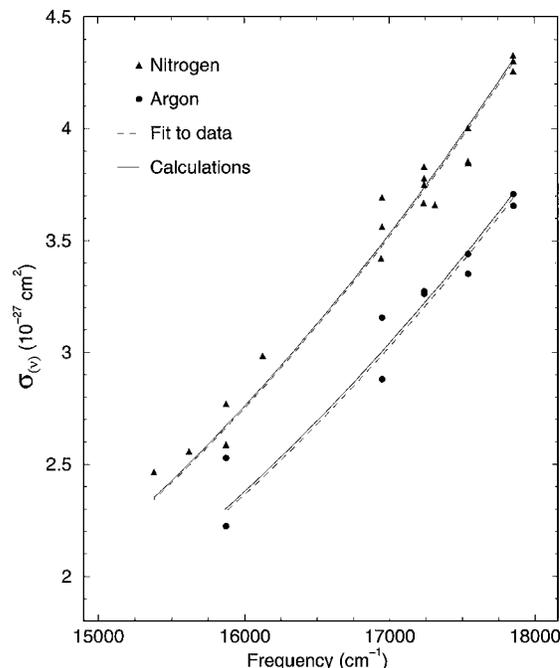

Fig. 2. Experimentally determined Rayleigh scattering cross sections for Ar and N$_2$ compared with calculations.

Table 1. Deduced Rayleigh Scattering Parameters $\bar{\sigma}_{th}$ and ϵ from Calculations and Experimentally Determined Values for $\bar{\sigma}_{exp}$[a]

Parameter	Ar	N_2	SF_6
$\epsilon \times 10^3$	61.5	62.4	41
$\bar{\sigma}_{th} \times 10^{45}$	20.04 (0.05)	23.00 (0.23)	183 (6)
$\bar{\sigma}_{exp} \times 10^{45}$	19.89 (0.14)	22.94 (0.12)	180 (6)

[a]The numbers in parentheses are the 1σ uncertainties.

are listed in Table 1. The dashed curves in Fig. 2 represent $\sigma_{(\nu)}$ as derived from the measurements.

In addition to the most-abundant atmospheric species, N_2, and a noble gas, Ar, SF_6, chosen for its extremely large Rayleigh scattering cross section resulting from its high refractive index, was also investigated. Very little is known about the refractive index of SF_6; in the literature only refractivities at 633 and 1300 nm have been reported.[14] Since SF_6 is a symmetrical octahedral, zero depolarization is assumed. From the data that we obtained, we extrapolate $\bar{\sigma}_{th} = 180 \ (6) \times 10^{-45}$ and $\epsilon = 0.041$. We estimate the error by taking into account the extrapolation error in ϵ. In Table 1 the value $\bar{\sigma}_{exp}$ as determined from the measured data is compared with the value following from the extrapolation.

The values for $\bar{\sigma}_{exp}$, obtained after several (weighted) fitting and data-analyzing procedures, allow for a comparison between the observed and the calculated values of the Rayleigh scattering cross section. Only then is a quantitative assessment of the small Rayleigh scattering phenomenon feasible. Finally, values for $\bar{\sigma}_{exp}$ are deduced with accuracies of $\approx 1\%$ for Ar and N_2 and 3% for SF_6.

Some remarks must be made about the assumption that in the present measurement a scattering cross section is determined. This assumption is valid only if absorption can be ruled out. In the Ar atom the first electronically excited state is in the vacuum-ultraviolet range and cannot give rise to absorption in the visible. In N_2, overtones of very weak quadrupole transitions will in principle occur in the visible, but these overtones will be too weak to cause observable absorption in the visible range or to affect the refractive index. In SF_6, with several active vibrational modes, visible absorption in electric-dipole-allowed overtone transitions could well be possible; however, in this study no such features are observed, and the Rayleigh scattering cross section is found to be consistent with predictions from the reported refractive index.[14]

Nonexponential decay of the observed CRD transients owing to laser bandwidth effects has hampered the application of pulsed-laser CRD to cross-section measurements of narrow features. The decay transient will remain exponential only if the bandwidth of the laser is much smaller than the width of the investigated extinction feature.[15] Since Rayleigh extinction is smooth and structureless, the 0.05-cm^{-1} bandwidth of the laser does not affect the results of this study.

The major result of this study is a quantitative verification of Rayleigh scattering cross sections for Ar and N_2 within the 1% experimental uncertainty. The present work represents, to the best of our knowledge, the first laboratory verification of a Rayleigh scattering cross section.

References

1. Lord Rayleigh, Philos. Mag. **47,** 375 (1899).
2. A. Bucholtz, Appl. Opt. **34,** 2765 (1995).
3. D. R. Bates, Planet. Space Sci. **32,** 785 (1984).
4. C. M. Penney, J. Opt. Soc. Am. **59,** 34 (1969).
5. L. V. King, Proc. R. Soc. London Ser. A **104,** 333 (1923).
6. E. R. Peck and D. J. Fisher, J. Opt. Soc. Am. **54,** 1362 (1964).
7. C. M. Penney, R. L. St. Peters, and M. Lapp, J. Opt. Soc. Am. **64,** 712 (1974).
8. N. J. Bridge and A. D. Buckingham, Proc. R. Soc. London Ser. A **295,** 334 (1966).
9. A. T. Young, J. Appl. Meteorol. **20,** 328 (1981).
10. R. Penndorf, J. Opt. Soc. Am. **47,** 176 (1957).
11. H. Naus and W. Ubachs, Appl. Opt. **38,** 3423 (1999).
12. M. D. Wheeler, S. M. Newman, A. J. Orr-Ewing, and M. N. R. Ashfold, J. Chem. Soc. Faraday Trans. **94,** 337 (1998).
13. P. M. Teillet, Appl. Opt. **29,** 1897 (1990).
14. D. Vukovic, G. A. Woolsey, and G. B. Scelsi, J. Phys. D **29,** 634 (1996).
15. P. Zalicki and R. N. Zare, J. Chem. Phys. **102,** 2708 (1995).